

A Test of the STIS CCD Flatfielding Accuracy on Small Scales

H. Ferguson

Space Telescope Science Institute, 3700 San Martin Drive, Baltimore, MD 21218

Abstract. This is a preliminary report on the reliability of STIS CCD flatfielding on small scales. The STIS CCD flat-field images are constructed from internal calibration lamp observations. As the calibration subsystem does not have the same focal ratio as the input path from the sky, shadows from dust particles on the detector face plate may not be corrected perfectly by the internal calibration. To test the repeatability of stellar photometry in the presence of these flatfield variations, observations of the core of the globular cluster 47 Tuc were made with the telescope offset repeatedly by small amounts between exposures. Preliminary results indicate that photometry is repeatable to better than 1%.

1. Introduction

With high throughput, good spatial resolution, and minimal charge-transfer effects, the STIS CCD may find use in many imaging programs. One of the factors that influences the achievable photometric accuracy is the quality of the flat fields, and the ability of calibrations carried out with the internal tungsten lamp to reproduce the detector response to external point sources.

The major small scale features in the STIS CCD flats are shadows of dust particles on the detector face plate (fig. 1). The most pronounced of these “dust motes” shows a 20% change in response from the center to the edge of the feature. Because the focal ratio of the calibration subsystem is different from that of the incoming beam from the telescope, it is unlikely that these features will be removed perfectly by the current pipeline flats.

2. Observations and Data Reduction

To test the quality of photometry with the current flats, and to provide data for testing various proposed improvements to the calibration (e.g. sky flats or modeling of the dust motes), observations were made of the center of the globular cluster 47 Tuc. Multiple images were taken with the telescope displaced in successive fine steps (0.02 arcsec in X and Y). The exposure times at each position were 3 seconds, and the exposures were CR-SPLIT to avoid contamination by cosmic rays. The proposal ID was 7641.

The 50CCD (clear aperture) data were calibrated using `calstis`, with the current (prelaunch) pipeline flats and the standard cosmic-ray rejection procedure. An example of a single reduced image is shown in fig. 2. A set of 376 stars brighter than magnitude $AB \sim 19$ and more than 50 pixels from the edge of the detector were identified using `daofind`, and their magnitudes were measured in a 3 pixel radius aperture in each of 18 individual frames using `daophot.phot`. Centroiding and background subtraction were done separately for each star in each frame.

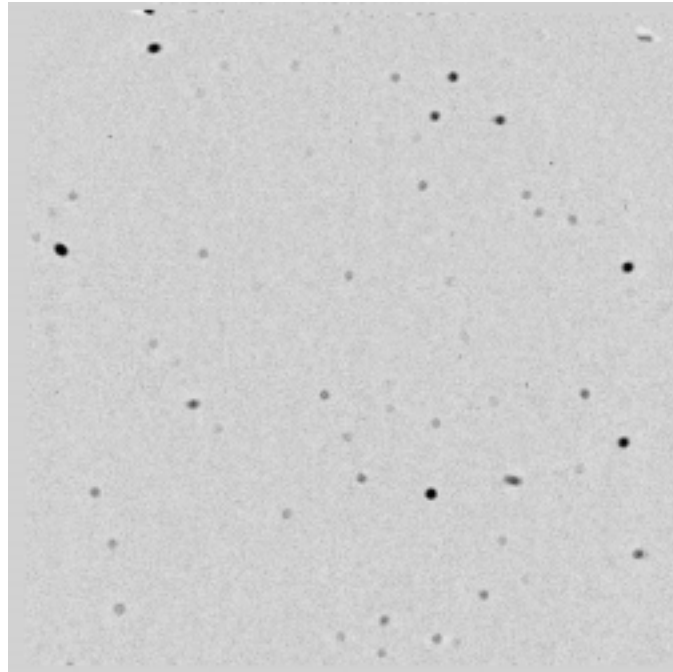


Figure 1. STIS 50CCD pipeline flat. This image was constructed from pre-flight measurements with the internal Tungsten calibration lamp. The circular features (dust motes) are caused by particles on the detector faceplate.

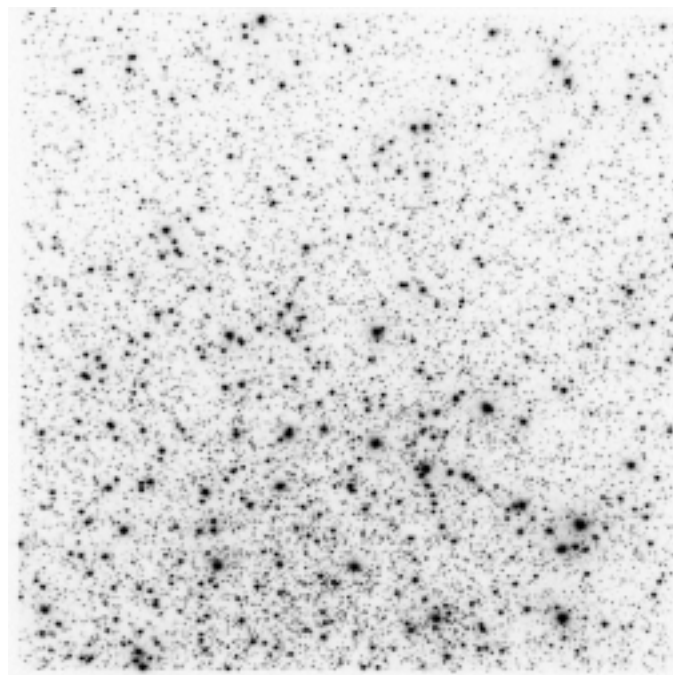


Figure 2. STIS 50CCD 3-second exposure of the center of 47 Tuc.

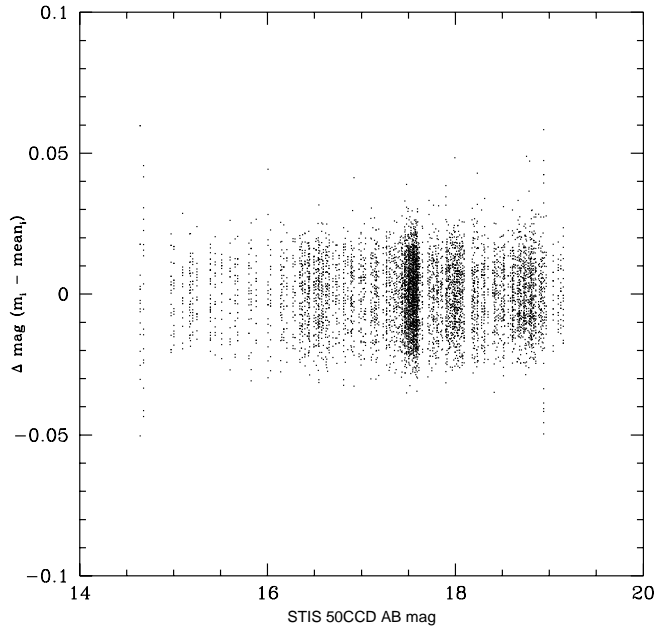


Figure 3. Photometric repeatability. The abscissa is the mean magnitude from the 18 measurements for each star. The ordinate is the difference between the individual measurements and the mean.

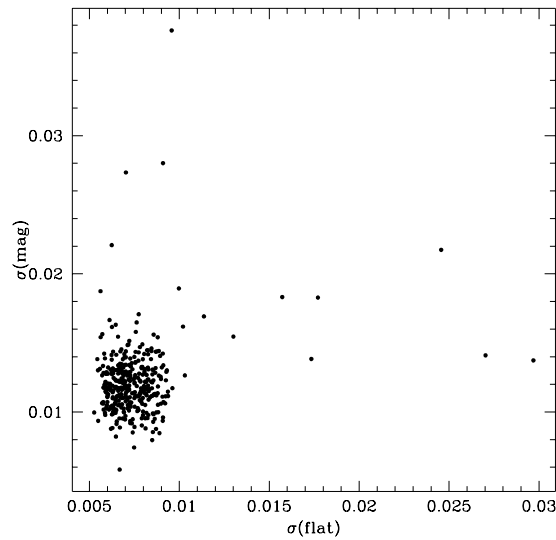


Figure 4. Photometric repeatability vs. stability of the flat. The abscissa shows the standard deviation of the pipeline flat for measurements in 0.2 arcsec radius apertures centered at the 18 positions of each star. The ordinate shows the standard deviation of the stellar magnitude measurements. The lack of a pronounced trend indicates that on average stars crossing pronounced features in the flat have similar photometric errors to those crossing smoother portions of the detector response.

3. Analysis

From pure counting statistics, we expect the standard deviation of the measured magnitudes to vary from 0.011 mag at $AB = 19$ to 0.003 mag at $AB = 16$. Figure 3 shows, for each of the 18×376 measurements, the difference between the star magnitude in each frame, and the mean magnitude of that star over all 18 frames. The standard deviation is less than 0.009 mag for all the images, and is typically ~ 0.007 mag. Small (< 0.02 mag) systematic shifts in zeropoint are seen in between frames, presumably due to telescope “breathing” which induces slow changes in the PSF with time.

To test whether features in the flat are influencing the photometry, the mean value of the flat in 2-pixel radius apertures was measured for each of the positions of the stars in the various images. For each star, we can then compute the standard deviation of the measured magnitude $\sigma(mag)$ and the standard deviation of the flat $\sigma(flat)$ over the range of positions sampled by the star. If uncertainties in the flat are dominating the photometric errors, one might expect to see the largest photometric errors where the flat showed the largest variation. Fig. 4 shows almost no correlation. Nevertheless, inspection of a few of the cases with the largest photometric residuals do show small (1-2 pixel) features in the flat that are the likely culprit. These are not dust motes, but probably something intrinsic to the detector such as charge traps.

4. Summary

The accuracy of the current STIS pipeline flats appears to be very good on scales of less than 4 arcsec. Inaccuracies in the flat induce rms photometric errors less (possibly substantially less) than 0.009 mag. Hence for point source photometry, photometric precision is likely to be governed by factors other than the accuracy of the flat, such as (1) changes in telescope and STIS focus with time (2) background subtraction in cases where there is a space or time-dependent background, and (3) corrections for overlapping PSFs in crowded fields.